

CORRESPONDENCE

Probing single-cell oxygen reserve in sickled erythrocytes via in vivo photoacoustic microscopy

To the Editor

Individuals with sickle cell disease (SCD) face ongoing risk of multi-organ ischemia resulting in chronic disability, frequent hospitalizations, and early mortality.¹ The relationship between hemoglobin (Hb) S polymerization, erythrocyte sickling, and tissue ischemia has been of great interest. Oxygen off-loading and increasing deoxy-Hb concentration promote HbS polymerization, the latter, which has been linked to early erythrocyte deformation or “reversible” sickling.² Eventually, severe polymerization weakens the cell membrane, leading to “irreversibly” sickled cells. Whether the degree of polymerization and the cell's morphologic state, in turn, influence oxygen binding and thus, tissue oxygen availability has been of interest, but technically challenging to study in patients.² Over two decades, Wang and colleagues³ developed an imaging platform, photoacoustic microscopy (PAM), which offers two unique aspects compared to other intravital microscopy systems: (1) high resolution in vivo *human* imaging using the cuticle as the window to a highly organized vascular bed capable of imaging single capillary loops, and (2) measurements of oxy- and deoxy-Hb levels within single capillaries and single erythrocytes. In this study, we aimed to: (1) characterize capillary morphology and hemodynamic/oxygen metabolic properties in the cuticle nailbed of individuals with SCD compared to healthy controls and (2) track single erythrocytes along the capillary loop to obtain measurements of erythrocyte elongation (ellipticity index, EI) and oxygen saturation before and after tissue oxygen exchange. We hypothesized that erythrocyte EI, as an index of HbS polymerization, would be associated with decreased arteriolar oxygen saturation and/or increased oxygen extraction fraction (OEF) across capillaries—representing compromised “oxygen reserve.”

Adult participants with SCD (HbSS) and controls (HbAA) were prospectively enrolled and excluded for recent hospitalization, chronic transfusion therapy, and history of stem cell transplant. Controls were excluded for any chronic medical disorder. Hb type was confirmed by peripheral blood electrophoresis. Written informed consent was obtained from all participants. PAM is a dual-wavelength optical resolution system with 3 μm lateral and 15 μm axial resolution (Figure S1). The blood absorption spectra from individuals with SCD previously have been found to be similar to that of healthy controls.⁴ The nailbed cuticle imaging procedure consisted of both wide-field and high-speed dynamic imaging. Capillary measurements included density, diameter, and tortuosity. Number and duration of erythrocyte pauses were measured from the spatiotemporal image and its frequency domain image.

Multiple hemo-metabolic parameters, calculated from both time-averaged, capillary measurements and single erythrocytes, included: blood velocity, oxygen saturation (sO_2), OEF, and relative metabolic rate of oxygen utilization (MRO_2). Single-cell PAM additionally yielded measurements of arteriolar (sO_2_{in}) and venular (sO_2_{out}) oxygen saturation, from which single-cell OEF was calculated. Elongation of single-cells, ellipticity index (EI), was measured as the mean EI of six frames for each flowing erythrocyte (Figure S2). Details of PAM imaging and statistical methods are described in the Appendix S1.

Ten adults with SCD (HbSS) and healthy controls (HbAA) underwent PAM cuticle imaging sessions, totaling 97 capillaries and 180 erythrocytes imaged (Table S1). Hb and hematocrit measured from peripheral blood correlated with cuticle Hb and hematocrit using PAM (Hb: $\rho = 0.825$, $p = .002$; Hct: $\rho = 0.800$, $p = .003$). Capillary diameter, density, and tortuosity were statistically increased in SCD versus healthy controls. Time-averaged capillary blood velocity was decreased in SCD versus controls: 62.5 $\mu\text{m/s}$ (51.0, 74.3) versus 69.8 $\mu\text{m/s}$ (63.6, 77.4), respectively ($p = .013$); capillary OEF was increased in SCD versus controls: 0.205 (0.150, 0.246) versus 0.147 (0.121, 0.188), respectively ($p = .049$); and capillary MRO_2 was similar in SCD versus controls: 49.9 arbitrary units (a.u.) (21.3, 60.9) versus 39.0 a.u. (26.1, 50.6), respectively ($p = .394$) (Figure S3).

Animal models of SCD have demonstrated the presence of red blood cell pauses, although the etiologies of pauses such as mechanical obstruction or endothelial adhesion are incompletely understood. Erythrocyte pause count was higher in SCD versus controls: 2 (2, 3) versus 1.5 (1, 2), respectively, ($p < .0001$). Pause duration was also higher in SCD versus controls: 14.6 s (10.3, 19.9) versus 7.0 s (4.5, 9.0), respectively, ($p < .0001$). Using a linear mixed-model to account for repeated measures within individuals, we evaluated the relationship between pause duration and capillary morphological and hemo-metabolic properties. Pause duration was inversely associated with blood velocity ($p = .009$), but not associated with OEF or capillary diameter. We also observed a direct association between pause duration and capillary tortuosity that approached significance ($p = .09$) (Figure S4).

PAM imaging can resolve individual erythrocytes, permitting a metric of elongated erythrocytes using “EI” (Figure S2). EI was increased in SCD versus controls: 0.201 (0.133, 0.245) versus 0.112 (0.075, 0.153), respectively ($p < .0001$) (Figure 1A). While the SCD cohort demonstrated a wider dynamic range of EI values, substantial overlap was seen across

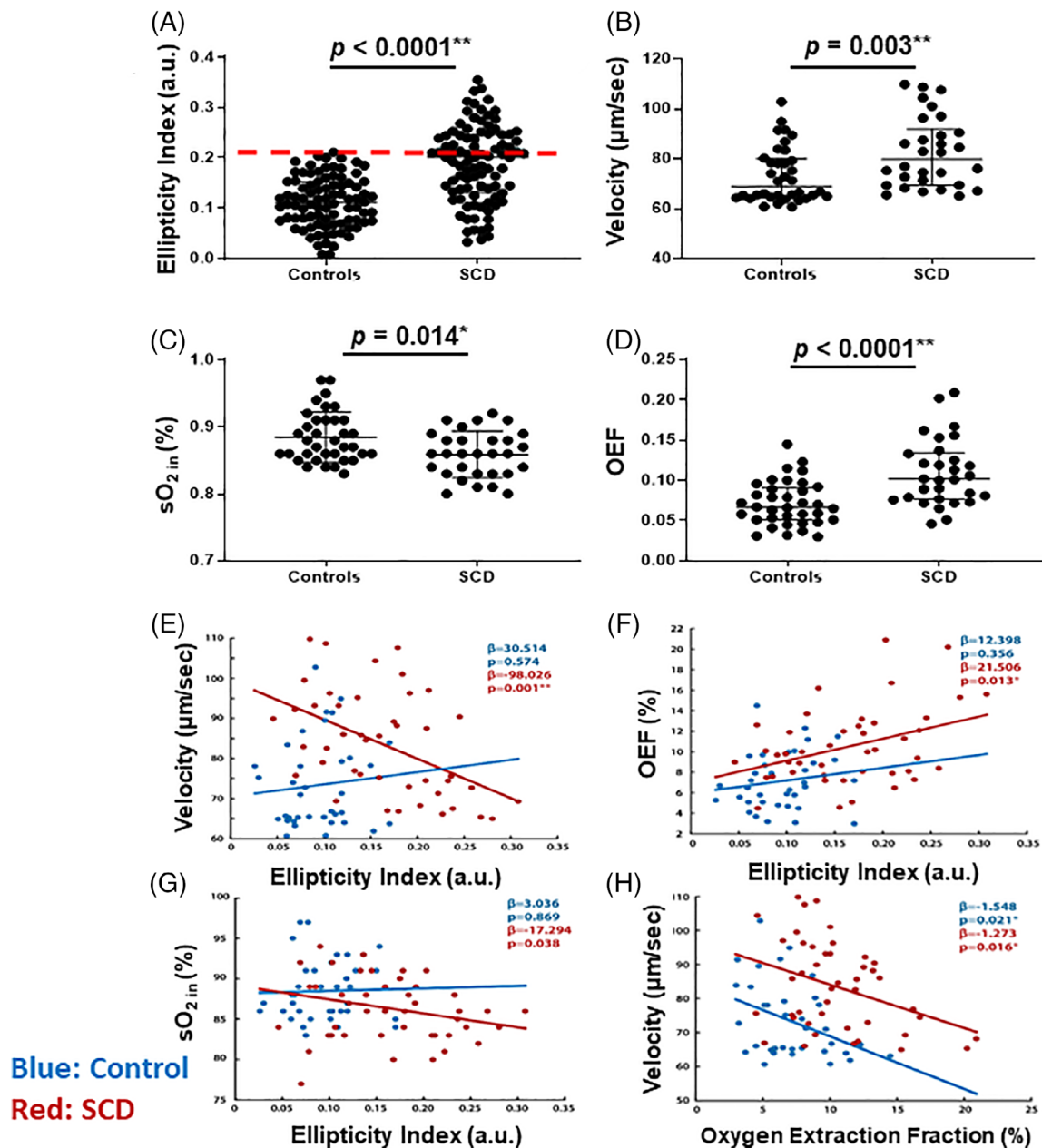


FIGURE 1 Single-cell hemo-metabolic parameters and ellipticity index (EI) as a predictor of single-cell blood flow and oxygenation in adults with SCD compared to controls. (A) Using PAM to measure the shape of single erythrocytes, EI, a metric of cellular anisotropy and deformation, was increased in the SCD cohort compared to controls ($p < .0001$). While the SCD cohort demonstrated a wider dynamic range of EI values, substantial overlap is seen across lower EI between the two cohorts, suggesting that SCD patients have a population of normal or near-normal shaped erythrocytes (below the red dashed line) as well as a subpopulation of elongated/sickled erythrocytes (above the red dashed line, indicating EI greater than two standard deviations above the mean EI from the control cohort). (B) Single-cell blood velocity was higher in SCD compared to controls ($p = .003$). During single-cell image acquisition, stalled erythrocytes were not included; therefore, this result represents an increase in velocity of red blood cells when the effect of pauses is unaccounted for. (C) Arteriolar oxygen saturation (sO_2 in) was lower in SCD compared to controls ($p = .014$) suggesting decreased oxygen delivery to the capillary bed in SCD. (D) In line with a decreased oxygen saturation in the arteriolar capillary bed, single-cell oxygen extraction fraction (OEF) was increased in the SCD cohort compared to controls ($p < .0001$). To evaluate the effect of erythrocyte ellipticity, as an index of Hb polymerization and sickling, on cellular flow and oxygen metabolism, mixed-model linear regression evaluated EI as a predictor of erythrocyte velocity, sO_2 in, and OEF. (E) Increasing EI predicted a decrease in blood velocity ($p = .001$) in SCD, but not in controls. (F) Consistent with this, increasing EI predicted an increase in OEF in SCD, but not in controls ($p = .013$). (G) Further, increasing EI non-significantly predicted a decrease in sO_2 in ($p = .038$) suggesting erythrocytes with greater ellipticity may have a lower oxygen content when entering the capillary. (H) Both in controls and SCD, OEF was inversely proportional to velocity suggesting that as the tissue's oxygen demands increase, erythrocyte velocity decreases allowing additional time for oxygen exchange, regardless of HbS polymerization and sickling. a.u. indicates arbitrary units. Raw p -values are reported. After adjusting for multiple testing with the Benjamini-Hochberg procedure, statistical significance was achieved, indicated as $*p < .05$ or $**p < .01$.

lower EI between the two cohorts, suggesting that SCD patients have a population of normal or near-normal shaped erythrocytes, consistent with the literature on peripheral blood.⁵ Moreover, the population of cells in the SCD cohort with increased EI extended beyond the EI distribution in controls, an observation consistent with HbS polymerization and sickling.

In contrast to velocity measurements using the time-averaged approach, mean single-cell blood velocity was higher in SCD versus controls: 79.8 $\mu\text{m/s}$ (69.4, 90.4) versus 68.9 $\mu\text{m/s}$ (64.7, 79.7), respectively ($p = .003$) (Figure 1B). During single-cell image acquisition, stalled erythrocytes were not included; therefore, this result likely represents an increase in cell velocity without accounting for the effect of pauses. Consistent with this, the measured velocities from the single-cell method for both control and SCD cohorts were higher than the velocities measured with the time-averaged method for capillaries.

Arteriolar oxygen saturation ($s\text{O}_2$ in) was lower in SCD versus controls ($p = .014$, Figure 1C) suggesting decreased oxygen availability to the capillary bed in SCD. Consistent with time-averaged results, single-cell OEF was increased in the SCD cohort versus controls: 0.101 (0.077, 0.133) versus 0.067 (0.051, 0.091), respectively ($p < .0001$) (Figure 1D). The finding of higher single-cell OEF is consistent with the observed anemia, diminished erythrocyte velocities, and reduced arteriolar oxygen saturation in patients with SCD, which suggests that greater oxygen extraction from individual erythrocytes is required to meet oxygen metabolic demand.

To examine the relationship between EI, as an index of Hb polymerization and sickling, and measures of erythrocyte velocity and oxygen metabolism, we performed mixed-model linear regression to examine EI as a predictor of velocity, $s\text{O}_2$ in, and OEF (Figure 1E–H). In SCD, but not in controls, an increase in EI was associated with slower erythrocyte velocity ($\beta = -98.0$, $p = .001$). Consistent with this, erythrocytes with greater EI were associated with increased OEF ($\beta = 21.5$, $p = .013$). Further, increased EI was associated with decreased $s\text{O}_2$ in ($\beta = -17.3$, $p = .038$). Erythrocyte velocity was also modeled in relation to OEF. Both in controls and SCD, individual erythrocyte OEF was inversely proportional to velocity indicating that erythrocyte OEF was increased with prolonged capillary transit time.

In this study, we used cuticle PAM to examine microstructural and physiological measures within capillaries and single-cells to advance our understanding of the pathophysiology underlying tissue ischemia in SCD. In addition to altered capillary architecture, individuals with SCD demonstrated reduced bulk flow velocity, increased OEF, more frequent erythrocyte pauses, and prolonged pause duration compared to controls. In single-cell measurements, we found that erythrocyte elongation (EI) was much higher in SCD versus controls. Moreover, EI distribution in patients with SCD was much broader, suggesting that a large subset of cells are elongated due to HbS polymerization (Figure 1A, above red dashed line). Previous studies have noted a spectrum of erythrocyte morphology and wide variation in the proportion of sickled cells (29%–43%).⁵

Indeed, we found higher EI in the SCD cohort predicted slower erythrocyte velocity, lower $s\text{O}_2$ in, and higher OEF, while these relationships were absent in controls. These findings suggest that sickled erythrocytes exhibit lower oxygen reserve than normally shaped erythrocytes, as indicated by both lower $s\text{O}_2$ in and increased OEF across the capillary loop, thus severe reductions in blood flow or $s\text{O}_2$ in would potentially place the tissue at risk of ischemia.

In summary, we found that increased EI, as a proposed index of polymerized HbS, was associated with distinct single-cell characteristics (velocity, arteriolar oxygen binding, and oxygen off-loading). This study was conducted in SCD patients who were not actively symptomatic, suggesting that baseline oxygen reserve (decreased $s\text{O}_2$ in and increased OEF) in patients with SCD may be compromised in a subset of erythrocytes. Increased OEF resulted in preserved MRO_2 , suggesting overall, a well-compensated metabolic state. Future PAM studies examining patients during vaso-occlusive crises may reveal an elevated proportion of “sickled” erythrocytes with elevated EI and decreased oxygen reserve. Such patients may be on the precipice of tissue infarction and could be identified for early intervention using PAM technology at the bedside.

The current work represents a proof-of-concept study suggesting that PAM technology may improve our understanding of the relationship between HbS polymerization, erythrocyte morphology, and tissue oxygen transport in SCD. Larger studies will be required to confirm our findings and examine covariates, which could further define these relationships. While our results demonstrate a link between EI and tissue oxygen availability, these relationships do not prove causality. Finally, we did not measure erythrocyte deformability, blood viscosity, or shear rates, which are known to be altered in patient with SCD and likely play a role in thrombosis and hemostasis.⁶ The potential influence of erythrocyte rheology on oxygen availability, however, should not impact the accuracy of hemo-metabolic measurements, nor minimize the cohort differences identified between SCD and controls.

ACKNOWLEDGMENTS

This work was supported by the National Institutes of Health R01HL129241 and RF1NS116565 (A.L.F.), R01NS094692, R37NS110699, U24NS107230 (J-M.L.), and R01GM113838 (A.D.).

AUTHOR CONTRIBUTIONS

Andria L. Ford and Hsun-Chia Hsu designed the experiment, collected the data, analyzed and interpreted data, and prepared the manuscript. Michael M. Binkley, Stephen Rogers, Toru Imai, and Konstantin Maslov analyzed and interpreted the data. Allan Doctor, Lihong V. Wang, and Jin-Moo Lee designed the experiment and analyzed and interpreted data. All authors critically reviewed and approved the final version of the manuscript.

CONFLICT OF INTERESTS

L. W. has a financial interest in Microphotoacoustics, Inc., CalPACT, LLC, and Union Photoacoustic Technologies, Ltd., which, however, did not support this work. The remaining authors do not have any competing interests.

DATA AVAILABILITY STATEMENT

The data that support the findings of this study are available on request from the corresponding author. The data are not publicly available due to privacy or ethical restrictions.

Andria L. Ford^{1,2} , Hsun-Chia Hsu³, Michael M. Binkley¹, Stephen Rogers⁴, Toru Imai³, Konstantin Maslov³, Allan Doctor⁴, Lihong V. Wang³, Jin-Moo Lee^{1,2,5}

¹Department of Neurology, Washington University School of Medicine, St. Louis, Missouri, USA

²Mallinckrodt Institute of Radiology, Washington University School of Medicine, St. Louis, Missouri, USA

³Caltech Optical Imaging Laboratory, Andrew and Peggy Cherng Department of Medical Engineering, Department of Electrical Engineering, California Institute of Technology, Pasadena, California, USA

⁴Department of Pediatrics, Center for Blood Oxygen Transport and Hemostasis, University of Maryland, Baltimore, Maryland, USA

⁵Department of Biomedical Engineering, Washington University School of Medicine, St. Louis, Missouri, USA

Correspondence

Jin-Moo Lee, Department of Neurology; Washington University School of Medicine; 600 South Euclid Avenue, Campus Box 8111; Saint Louis, MO 63110, USA.
Email: leejm@wustl.edu

Lihong V. Wang, Caltech Optical Imaging Laboratory, Andrew and Peggy Cherng Department of Medical Engineering, California Institute of Technology, 1200 E. California Blvd., MC 138-78 Pasadena, CA 91125, USA.
Email: lihong@caltech.edu

Present address

Hsun-Chia Hsu, Center for Devices and Radiological Health, U.S. Food and Drug Administration, Silver Spring, Maryland, USA

Dr. Andria L. Ford and Dr. Hsun-Chia Hsu contributed equally and are designated as co-first authors.

Dr. Jin-Moo Lee and Dr. Lihong V. Wang contributed equally and are designated as co-senior authors.

ORCID

Andria L. Ford  <https://orcid.org/0000-0003-0605-8943>

REFERENCES

1. Piel FB, Steinberg MH, Rees DC. Sickle cell disease. *N Engl J Med*. 2017;376(16):1561-1573.
2. Eaton WA, Hofrichter J. Hemoglobin S gelation and sickle cell disease. *Blood*. 1987;70(5):1245-1266.
3. Hsu HC, Wang L, Wang LV. In vivo photoacoustic microscopy of human cuticle microvasculature with single-cell resolution. *J Biomed Opt*. 2016;21(5):56004.
4. Nahavandi M, Nichols JP, Hassan M, Gandjbakhche A, Kato GJ. Near-infrared spectra absorbance of blood from sickle cell patients and normal individuals. *Hematology*. 2009;14(1):46-48.
5. Alvarez O, Montague NS, Marin M, O'Brien R, Rodriguez MM. Quantification of sickle cells in the peripheral smear as a marker of disease severity. *Fetal Pediatr Pathol*. 2015;34(3):149-154.
6. Gillespie AH, Doctor A. Red blood cell contribution to hemostasis. *Front Pediatr*. 2021;9:629824.

SUPPORTING INFORMATION

Additional supporting information may be found in the online version of the article at the publisher's website.